

# Using Single-Molecule Approaches To Study Archaeal DNA-Binding Protein Alba1

Yen-Wen Lu,<sup>†</sup> Tao Huang,<sup>‡</sup> Cheng-Ting Tsai,<sup>‡</sup> Yu-Yung Chang,<sup>§</sup> Hung-Wen Li,<sup>‡</sup> Chun-Hua Hsu,<sup>§,||</sup> and Hsiu-Fang Fan<sup>\*,†</sup>

<sup>†</sup>Department of Life Sciences and Institute of Genome Sciences, National Yang-Ming University, 112 Taiwan

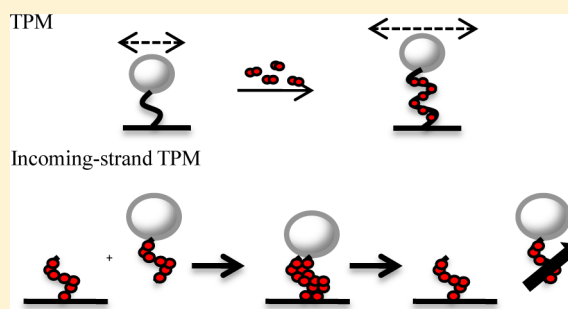
<sup>‡</sup>Department of Chemistry, National Taiwan University, 106 Taiwan

<sup>§</sup>Department of Agricultural Chemistry, National Taiwan University, 106 Taiwan

<sup>||</sup>Center for Systems Biology, National Taiwan University, 106 Taiwan

## Supporting Information

**ABSTRACT:** Thermophilic and hyperthermophilic archaea have one or more copies of the *Alba* gene, which encodes Alba, a dimeric, highly basic protein that binds cooperatively to DNA. However, the functions of Alba and how it interacts with DNA remain unclear. In this study, we have used single-molecule tethered particle motion (TPM) and optical tweezers (OT) experiments to study the interactions between DNA molecules and Alba1. When Alba1 binds to double-stranded DNA, the Brownian motion (BM) amplitude for DNA tethers increases continuously, suggesting that Alba1 binds cooperatively. The OT study confirmed that a 5-fold increase in the persistence length of the Alba1 nucleoprotein filament is the major factor causing the increase in the BM amplitude for DNA tethers, while the contour length remained mostly unchanged. Moreover, the rate of the increase in the BM amplitude and the BM plateau value are both DNA length-dependent, indicating that the number of Alba1 initiation binding sites increases as the DNA becomes longer. Using the incoming-strand TPM experiment to monitor the interaction between Alba1 nucleoprotein filaments, we found that significant dimer–dimer contacts between two Alba1 nucleoprotein filaments are present, and the interaction is regulated by the concentration of Alba1.



Genomic information is maintained by architectural DNA-binding proteins, which have been shown to be essential for regulating gene expression. In eukaryotes, it is well-known that histone octamers wrap approximately 147 bp DNA molecules into the nucleosome structure.<sup>1</sup> In eubacteria, dsDNA-binding proteins, such as HU, have been shown to compact DNA.<sup>2</sup> An informational pathway similar to that of eukarya has been found in archaea. However, a histone-like protein that wraps an approximately 70 bp DNA molecule into a tetrameric nucleosome is found only in a subset of archaea.<sup>3</sup>

The small DNA-binding protein Alba1, also known as Sac10b or Sso10b, was found to be an abundant dimeric protein in *Sulfolobus shibatae*, comprising 4% of the total soluble protein.<sup>4</sup> This protein is conserved in most sequenced archaeal genomes,<sup>5</sup> binds to double-stranded DNA (dsDNA) without sequence specificity,<sup>4,6</sup> and possesses acetylation-regulated DNA binding affinity.<sup>6,7</sup> This evidence supports the hypothesis that Alba1 can play an important role in chromatin organization in archaea. Electron microscopy (EM) data have shown that purified Alba1 from *Sulfolobus acidocaldarius* binds to dsDNA without causing significant compaction,<sup>8</sup> contradicting the hypothesis that Alba1 is a potential architectural DNA-binding protein that compacts the chromatin in archaea. However, the presence of two distinct copies of the *Alba* gene,

*Alba1* and *Alba2*, and the strikingly different DNA compaction structures produced by these two Alba proteins suggest that an alternative DNA packaging model is required.<sup>9–11</sup> Moreover, nuclear magnetic resonance (NMR) and crystal structural experiments have identified dimer–dimer contacts between two Alba nucleoprotein filaments, suggesting that Alba nucleoprotein filaments can interact with each other through these dimer–dimer contacts to condense DNA molecules.<sup>10,12</sup> Alba is evolutionarily conserved and is important for maintaining DNA integrity.<sup>13</sup> How Alba1 interacts with duplex DNA molecule and what the detailed kinetics is have not been well studied.

Single-molecule techniques can elucidate individual interactions that cannot be detected with conventional biochemical techniques. Therefore, single-molecule methods offer valuable information about the details of the molecular mechanisms associated with enzyme functions.<sup>14–21</sup> Using atomic force microscopy (AFM) and optical trapping techniques, Laurens et al. recently found that Alba can shape DNA by bridging and stiffening the DNA strands.<sup>22</sup> It has been reported that there is

**Received:** August 2, 2013

**Revised:** September 10, 2013

**Published:** October 4, 2013



a significant increase in the persistence length of Alba1 nucleoprotein filaments as the Alba1 concentration increases. Moreover, there are significantly different protein–protein interactions when the two Alba variants, Alba1 and Alba2, are compared.<sup>22</sup> The tethered particle motion (TPM) experiment, an easily used and nearly force-free tool, has been used to probe interactions between proteins and individual DNA molecules.<sup>23–27</sup> In this study, a single-molecule TPM experiment was used to investigate the detailed interactions between Alba1 and individual DNA molecules in real time. A significant increase in the Brownian motion (BM) amplitude was observed. In addition, the kinetic assembly process can be determined by analyzing the BM time trace. We also used a homemade optical tweezers (OT) setup to confirm that a significant increase in persistence length, without a detectable change in the contour length of the Alba1 nucleoprotein filament, is the major factor causing the significant increase in the BM amplitude for the DNA tether. Moreover, dimer–dimer contacts between two Alba1 nucleoprotein filaments were observed on the basis of the incoming-strand TPM experiment, consistent with previous NMR, crystal structure, and, more recently, single-molecule data.<sup>10,12,22</sup> The single-molecule experiments developed here offer alternative ways to investigate the properties of archaeal DNA-binding protein Alba1.

## MATERIALS AND METHODS

**Proteins and DNA Substrates.** The *Sulfolobus solfataricus* P2 (EMBL entry CAC23286) *Alba* (*Sso10b*) gene was cloned into the pET-30 (Novagen) vector and expressed in *Escherichia coli* BL21(DE3). The purification procedure has been described previously.<sup>28</sup> Briefly, protein expression was induced by the addition of 0.4 mM isopropyl  $\beta$ -D-thiogalactoside (IPTG) at 37 °C for 3 h. The cells were collected by centrifugation, resuspended in lysis buffer [50 mM Tris-HCl (pH 7.5) and 100 mM NaCl], and disrupted by sonication. The lysate was then centrifuged at 40000g. The supernatant was heated to 338 K for 10 min in a water bath, and the denatured proteins were precipitated by centrifugation at 40000g. The supernatant was loaded into an SP-Sepharose high-performance 26/10 column (Hi-Load, GE Healthcare). A gradient from 0 to 1.0 M NaCl in buffer A was used to elute the cationic proteins. Fractions corresponding to a distinct absorbance peak were analyzed by sodium dodecyl sulfate–polyacrylamide gel electrophoresis (SDS–PAGE) and shown to contain essentially homogeneous Alba1 protein. The absence of the first methionine residue has been reported by using electrospray (ES) mass spectrometry (MS).<sup>29</sup>

Various DNA molecules (211, 427, 836, and 1551 bp in length) were prepared by polymerase chain reaction (PCR) using digoxigenin-labeled and biotin-labeled primers and pBR322 (NEB) as a template. The DNA molecule used in the OT experiment (6123 bp in length) was prepared by PCR using digoxigenin-labeled and biotin-labeled primers and M13mp18 (NEB) as a template. The primer sequences are listed in Table 1.

**Single-Molecule TPM Measurement and Data Analysis.** The reaction samples and chambers were prepared as previously described.<sup>23,24,26,27</sup> The experiment was performed under an inverted optical microscope (IX-71, Olympus, 100 $\times$  objective with NA = 1.40) using a differential interference contrast (DIC) imaging system at 22 °C. The experimental images were recorded continuously with an analog camera

**Table 1. Primer Sequences Used To Obtain the Experimental DNA Molecules**

DNA substrate	template	primer sequence
211 bp dsDNA	pBR322	Dig 5' CGTCACCCTGGATGCTGTAG Bio 5' GGCTCCAAGTAGCGAAGCG
427 bp dsDNA	pBR322	Dig 5' ACTACGATACGGGAGGGC Bio 5' CGGATGGCATGACAGTAAG
836 bp dsDNA	pBR322	Dig 5' CGTCACCCTGGATGCTGTAG Bio 5' CGTAGCCCAGCGCGTCG
1551 bp dsDNA	pBR322	Dig 5' CGTCACCCTGGATGCTGTAG Bio 5' GCAGATCCGGAACATAATGG
4195 bp dsDNA	pBR322	Dig 5' GGCGTGGGTATGGTGGA Bio 5' GGCTCCAAGTAGCGAAGCG
6123 bp dsDNA	M13mp18	Dig 5' TGCCACCTTTTCAGCTCG Bio 5' AGTGTAAGCCTGGGGTG

(Newvicon-70, frame interval of 33 ms). A mercury lamp was used as an illuminator to enhance image contrast. All data analysis and criteria followed previously described procedures.<sup>23,24,26,27</sup> Only those molecules with a BM amplitude within the 95% confidence level (CL) by a 40-frame averaging window before the addition of Alba1 were chosen as bare DNA molecules and used for further analysis. Molecules that stuck to the glass surface (with a BM amplitude of <10 nm) for more than five points or that exhibited distorted movement (the ratio of BM amplitude on the x-axis to BM amplitude on the y-axis is outside the range of 0.8–1.2) at any time were excluded.

The nucleation time of Alba1 on the DNA molecule was pooled into a duration histogram and fit with a single-exponential decay algorithm using the following formula:

$$y = A_1 \times e^{-k_1 t} \quad (1)$$

where  $A_1$  and  $k_1$  are the fitting parameters determined by Origin 8.0. The rate of extension of Alba1 on the DNA molecule was obtained by analyzing the increase in the BM amplitude using a least-squares linear fitting algorithm written in Origin 8.0. The data analysis procedure followed the previous described algorithm.<sup>25</sup>

Each DNA molecule was labeled with digoxigenin and biotin at the 5' end and immobilized onto an anti-digoxigenin-coated coverslip surface. A streptavidin-coated 200 nm polystyrene bead was attached at the other end as a reporter. The interaction between Alba1 and an individual DNA molecule was initiated by adding the complete reaction solution containing specific concentrations of Alba1 (100 nM, 1  $\mu$ M, and 10  $\mu$ M) prepared in reaction buffer [20 mM MES (pH 6.5), 100 mM potassium glutamate, 1 mM magnesium chloride, and 1 mg/mL bovine serum albumin (BSA)]. The reaction chamber has two open inlets, and the reaction solution was added through one of two open inlets by using a Pipetman. All experiments were performed at room temperature (22 °C).

For incoming-strand TPM, a 211 bp DNA molecule was immobilized on the anti-digoxigenin-coated coverslip surface. The reaction was initiated once 30  $\mu$ L of reaction solution containing 1 nM 211 bp DNA molecules, labeled with 200 nm polystyrene beads and incubated with a specific concentration of Alba1 (10  $\mu$ M or 100 nM) prepared in reaction buffer [20 mM MES (pH 6.5), 100 mM potassium glutamate, 1 mM magnesium chloride, and 1 mg/mL BSA], had been loaded into the reaction chamber. The appearance of tethers indicated that two dsDNA molecules were pulled together by the dimer–dimer contacts between two Alba1 nucleoprotein filaments.

The stability of the dimer–dimer contacts is represented by the lifetime of these tethers, and the lifetime histogram was fit to a single-exponential decay model by Origin 8.0.

### Single-Molecule OT Measurement and Data Analysis.

For the force-extension experiment, a homemade OT was used.<sup>30</sup> A 1064 nm laser was used to apply the trapping force to the tethered DNA molecules labeled with polystyrene beads with a diameter of 1040 nm (Bangs Lab). The trapping force was controlled with the rotational half-wave plate and monitored by checking the quadrant photodiode (QPD) voltage. The nanometer movement was controlled by a three-dimensional piezo stage (Madcity Lab). The force–extension curves obtained from bare DNA molecules or Alba1 nucleoprotein filaments (6123 bp in length) were fit to the wormlike chain (WLC) model written in Matlab.<sup>31</sup>

$$\frac{FP}{k_B T} = \frac{1}{4} \left( 1 - \frac{l}{L_0} \right)^{-2} - \frac{1}{4} + \frac{l}{L_0} \quad (2)$$

where  $F$  represents the force applied to the DNA molecules,  $P$  and  $L_0$  represent the persistence length and the contour length, respectively,  $l$  represents the extension length under a specific force, and  $k_B$  and  $T$  are the Boltzmann constant and temperature, respectively. We mainly analyzed the force–extension curve in the force range of 0.1–2.5 pN and masked the fluctuation region of the low-force part for clarification.<sup>32</sup>

## RESULTS

**Monitoring the Interaction between Alba1 and the dsDNA Molecule Using the TPM Experiment.** Herein, a single-molecule TPM was developed to monitor the interaction between Alba1 and an individual DNA molecule in real time. The DNA molecule (211 bp in length) was immobilized on an anti-digoxigenin-coated coverslip, and the other end of the DNA was labeled with a 200 nm polystyrene bead. The BM of the tethered bead was monitored using DIC microscopy. The reaction was initiated by loading 30  $\mu$ L of a mixed solution containing 10  $\mu$ M Alba1 prepared in reaction buffer [20 mM MES (pH 6.5), 100 mM potassium glutamate, 1 mM magnesium chloride, and 1 mg/mL BSA]. There are two possible scenarios in which Alba1 binds to the DNA. First, an increase in the BM amplitude indicates the extension or stiffening of the Alba1 nucleoprotein filament [Figure 1A, (i)]. Second, a decrease in the BM amplitude indicates Alba1-mediated DNA condensation [Figure 1A, (ii)].

A control experiment performed with the 211 bp DNA molecules with reaction buffer in the absence of Alba1 showed no significant change in the BM time trace [Figure 1B, (i)]. The addition of 10  $\mu$ M Alba1 caused an increase in the BM amplitude of the DNA molecules to a steady plateau [Figure 1B, (ii)], indicating that the DNA filament was extended or became stiffer after Alba1 binding. We found that there was no significant compaction of Alba1 nucleoprotein filaments at high Alba1 concentrations, which is consistent with previous experimental results.<sup>7–9</sup> An extensive buffer wash did not remove the Alba1 from the DNA molecules, indicating a strong DNA binding affinity for the Alba1 [Figure 1B, (ii)]. Among all of the 113 analyzed DNA molecules, an increase in the BM value from  $20.8 \pm 3.2$  nm to an average value of  $26.1 \pm 5.4$  nm, exhibiting a significant difference in the 99.9% CL, was observed for the 211 bp DNA molecules in response to the addition of 10  $\mu$ M Alba1 [Figure 1C, (i) and (ii)]. The same experiments were then performed for the 211 bp DNA

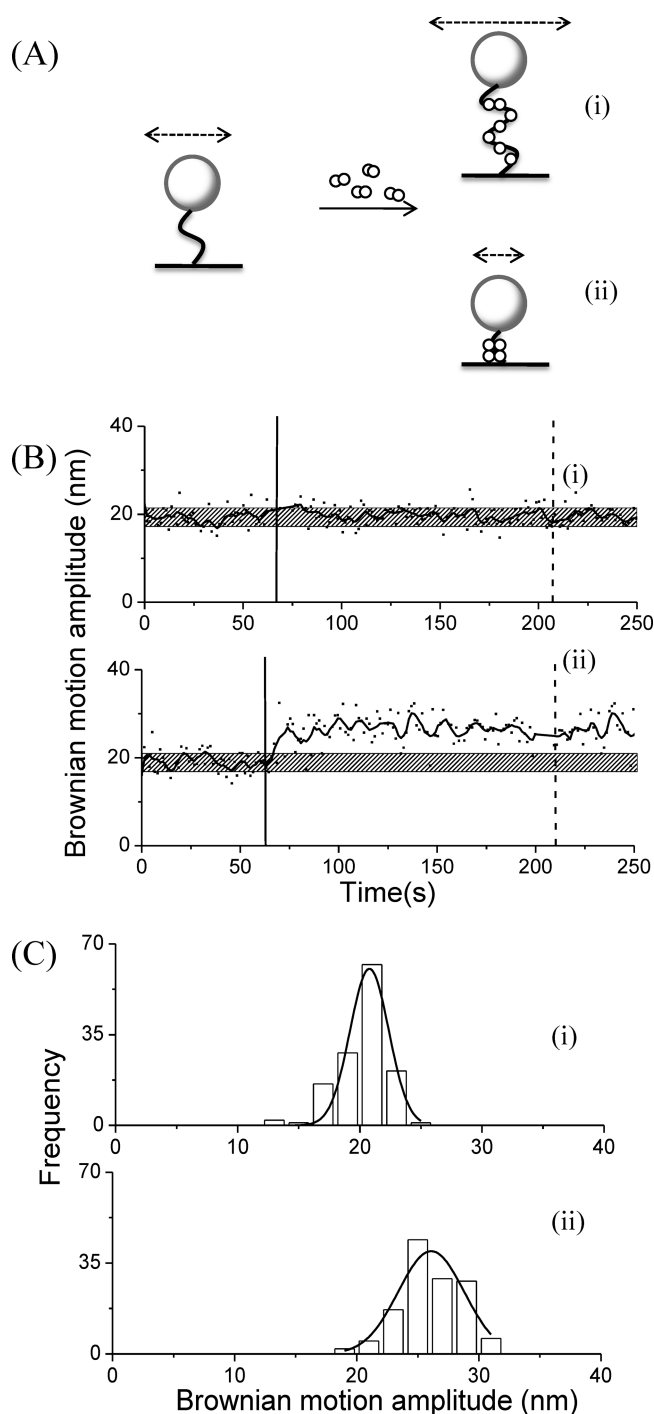


**Figure 1.** Tethered particle motion experiment investigating the interaction between Alba1 and DNA molecules. (A) Possible reaction mechanism between Alba1 and DNA molecules. (i) Alba1-induced DNA molecule extension is reflected as an increase in the BM amplitude. (ii) Alba1-induced DNA molecule condensation is represented as a decrease in the BM amplitude. The cartoons shown here illustrate the experimental procedure. The white sphere represents the streptavidin-labeled 200 nm polystyrene bead. The white spots represent the Alba1 molecules. The black curve represents the DNA molecules. The dashed double-headed line represents the BM amplitude. (B) (i) Control experiment showing the BM time trace for the 211 bp DNA molecule in the reaction buffer. (ii) BM time trace for the 211 bp DNA molecule in response to the addition of 10  $\mu$ M Alba1. The hatched bar represents the expected BM amplitude for the 211 bp DNA molecule at a 95% confidence level (CL). The black line indicates the addition of a reaction solution with Alba1. The

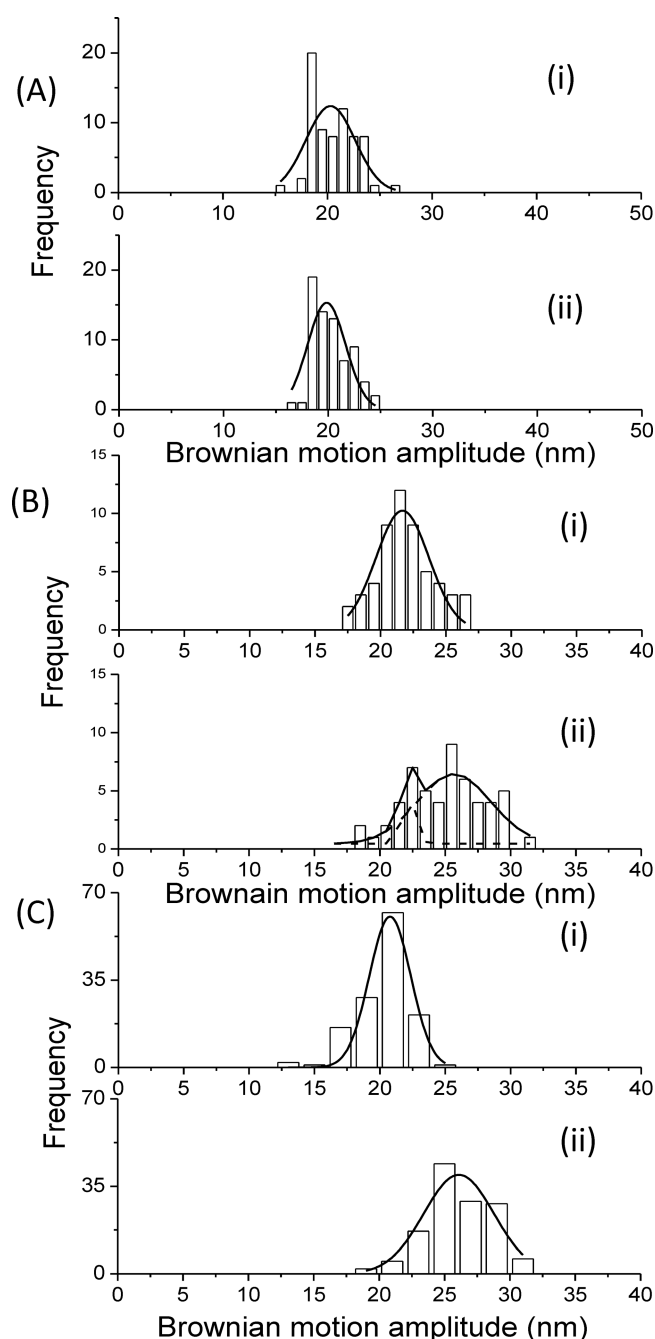


Figure 1. continued

dashed line indicates the extensive buffer wash (100  $\mu$ L of reaction buffer without Alba1). (C) (i) Histogram of the BM amplitude obtained from 211 bp DNA molecules in reaction buffer ( $20.8 \pm 3.2$  nm at a 95% CL, with 131 molecules). (ii) Histogram of the BM amplitude obtained from 211 bp DNA molecules incubated with 10  $\mu$ M Alba1 for 15 min ( $26.1 \pm 5.4$  nm at a 95% CL, with 131 molecules).

molecules at different Alba1 concentrations (Figure 2). At Alba1 concentrations of <100 nM, there was no detectable change in the BM time trace (data not shown). The reported  $K_d$  for Alba1 on dsDNA is approximately 56–200 nM,<sup>9</sup> and the Alba1 binding percentage along the dsDNA molecule is proportional to the concentration of Alba1 at relatively low Alba1 concentrations.<sup>22</sup> The undetectable change in the BM amplitude for the DNA molecules in response to 100 nM Alba1 could be due to either an overestimation of the concentration of Alba1 or the presence of inactive contaminant proteins. Moreover, the interaction between Alba1 and the DNA molecules was determined by the change in the BM amplitude. We cannot rule out the possibility that the overestimation in the required Alba1 concentration was caused by poor resolution of the BM change point during TPM. However, the interaction between Alba1 and dsDNA becomes easily detectable once the concentration of Alba1 is above the reported  $K_d$  (Figure 2). The BM plateau value in each BM time trace for DNA molecules in response to the different Alba1 concentrations increased to a similar value. Only the percentage of DNA molecules that in response to Alba1 formed Alba1 nucleoprotein filaments increased as the Alba1 concentration was increased (Figure 2). It suggests that the DNA molecule is fully assembled by the Alba1 proteins in the status with a BM amplitude of  $26.1 \pm 5.4$  nm once the Alba1 concentration is above the  $K_d$  and confirms the highly cooperative nature of Alba1.

Because a significant change in the BM amplitude was observed for the DNA molecule in response to 10  $\mu$ M Alba1, the same experiments were also performed on DNA molecules of different lengths without sequence specificity (427, 836, and 1551 bp) using 10  $\mu$ M Alba1 prepared in the same reaction buffer. A significant increase in the BM amplitude after the addition of 10  $\mu$ M Alba1 was observed for all DNA molecules regardless of length, as illustrated in the representative time traces (Figure S1A–C of the Supporting Information). This confirms that Alba1 binds to DNA without sequence specificity.<sup>4,6</sup> Some theoretical models were derived to interpret the Brownian motion amplitude of the TPM experiment, and a polynomial relationship with a negligible high-order coefficient was obtained, suggesting an approximately linear property for short DNA molecules.<sup>33,34</sup> Even though the 1551 bp DNA molecule is included here, the empirical TPM calibration curves obtained for the bare DNA molecule and Alba1 nucleoprotein filaments appear to be linear with  $R^2$  values of 0.99 and 0.96, respectively (Figure 3). Interestingly, a 2-fold increase in the slope of the BM amplitude versus the tethered DNA length was observed for Alba1 nucleoprotein filaments compared with that of bare DNA molecules. It has been known that two factors will affect the BM amplitude of a tether molecule: persistence length and contour length.<sup>25</sup> It has been reported that the persistence length of the Alba1 nucleoprotein filament increases, while the contour length remains the same within



**Figure 2.** Histogram of the BM amplitude for 211 bp DNA molecules before and after incubation with different concentrations of Alba1. (A) BM amplitude distribution histograms (i) before and (ii) after incubation with 100 nM Alba1. The histograms were fit to a single-Gaussian distribution model with average BM values of  $20.3 \pm 4.7$  nm in the absence of Alba1 and  $19.9 \pm 3.6$  nm in the presence of Alba1 ( $N = 83$ ). (B) BM amplitude distribution histograms (i) before and (ii) after incubation with 1  $\mu$ M Alba1. The histograms were fit to a single-Gaussian distribution model and a two-Gaussian distribution model with average BM values of  $21.7 \pm 4.0$  nm in the absence of Alba1 and  $22.2 \pm 1.0$  and  $25.7 \pm 5.6$  nm in the presence of 1  $\mu$ M Alba1 ( $N = 55$ ). (C) BM amplitude distribution histograms (i) before and (ii) after incubation with 10  $\mu$ M Alba1. The histograms were fit to a single-Gaussian distribution model with average BM values of  $20.8 \pm 3.2$  nm in the absence of Alba1 and  $26.1 \pm 5.4$  nm in the presence of 10  $\mu$ M Alba1. The error bars express the 95% CL ( $N = 131$ ).

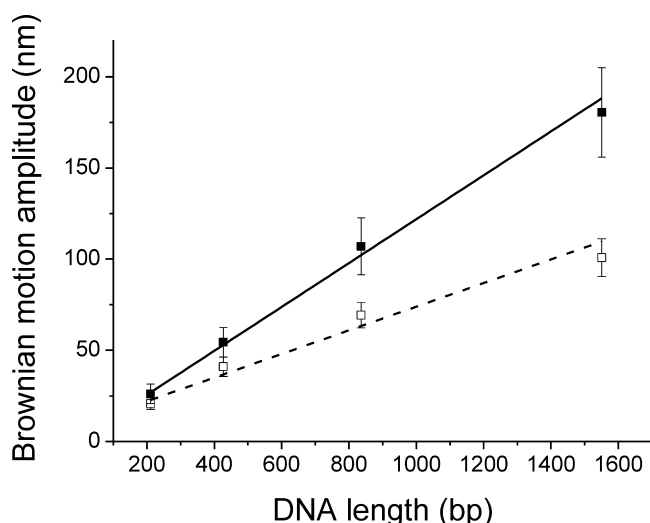


**Figure 3.** Calibration curve for BM amplitude vs DNA tether length. The relationship between the BM amplitude of the DNA molecules labeled with a 220 nm polystyrene bead, which is represented by the standard deviation of centroid positions using subsequent 40-frame images, and the DNA tether length is linear. The black squares represent data for Alba1-bound DNA molecules. The white squares represent data for bare DNA molecules. The distributions were fit to straight lines using equations  $y = 0.12x + 1.56$  ( $R^2 = 0.99$ ) and  $y = 0.06x + 9.07$  ( $R^2 = 0.96$ ), respectively. The error bar expresses the 68% CL.

an Alba1 concentration range of 1–2000 nM.<sup>22</sup> To confirm which factor contributes to the significant increase in the BM amplitude observed here at 10  $\mu$ M Alba1, a homemade OT was used to study the elasticity of Alba1 nucleoprotein filaments.

**Assessing the Elasticity of an Alba1 Nucleoprotein Filament Using OT.** In this force–extension experiment, the individual surface-immobilized and bead-labeled DNA molecules were extended by a stretching force that was introduced by a 1064 nm laser system controlled with an intensity modulation setup. We then varied the stretching force by moving the piezo stage. The pulling geometry was adopted from a previously reported setup<sup>35</sup> and is shown in Figure S2 of the Supporting Information. The DNA extension length ( $l$ ) was determined by the bead’s scattering signal, which was captured by a QPD. The QPD voltage signal was then converted to distance on a nanometer scale.

We then studied the elasticity of 6123 bp dsDNA molecules in the absence and presence of 10  $\mu$ M Alba1 [after incubation for 15 min [Figure S2B of the Supporting Information, (i) and (ii)]]. The differences in the force–extension curves suggested that there had been a change in the elasticity of the Alba1 nucleoprotein filaments. The determined contour length of  $2058 \pm 16$  nm and persistence length of  $203 \pm 24$  nm for the Alba1 nucleoprotein filament (Figure S2B of the Supporting Information) are similar to previously reported values.<sup>22</sup> The contour length of the Alba1 nucleoprotein filament ( $2058 \pm 16$  nm) is approximately the same as that of the expected B-form dsDNA molecules (2081 nm) within experimental error, which is also consistent with previous structural studies.<sup>8,9</sup>

We surveyed 25 Alba1 nucleoprotein filaments [Figure S2C of the Supporting Information, (i)]. The persistence lengths of the Alba1 nucleoprotein filaments were higher than those of the bare B-form dsDNA and showed a distribution across a range [Figure S2C of the Supporting Information, (ii)]. On average,

an Alba1 nucleoprotein filament was approximately 5-fold stiffer than the B-form dsDNA. In contrast, the contour lengths of these filaments were similar to those of the bare dsDNA, with a similar distribution. This finding confirmed that Alba1 alters the stiffness of the filament but not the contour length. The wider persistence length distribution in the Alba1 nucleoprotein filaments was likely due to differences in the coating percentages of the nucleoprotein filaments under tension.

**Kinetic Analysis of the Interaction between Alba1 and Individual DNA Molecules.** Two parameters, the nucleation time and extension rate, can be defined for the typical BM time trace of the Alba1 assembly process. First, the nucleation time was defined as the dwell time between the addition of Alba1 and the time point at which there is a significant change in the BM amplitude (marked with the double-headed line in Figure 4A). This reflects the DNA binding affinity, the association rate constant ( $k_{on}$ ), of Alba1. Second, the extension rate was defined as the slope of the BM amplitude increase at a given time (marked as the dashed line in Figure 4A), which reflects the polymerization ability of Alba1. The nucleation time is too short to be accurately measured once the DNA molecules become longer. Therefore, only the nucleation time for the 211 bp DNA molecules can be accurately determined. The nucleation times were pooled and fit to a single-exponential decay, with an average nucleation time of  $7.4 \pm 0.4$  s for 211 bp DNA (Figure 4B).

The same experiments and analysis procedures were applied to DNA molecules of different lengths at 1  $\mu$ M Alba1. Longer DNA molecules had shorter nucleation times (Figure S3 of the Supporting Information), which is in agreement with the prediction that the nucleation time depends on the number of available nucleation sites. The extension rate was determined by applying a linear fit to the increasing BM region in each BM time trace (marked in Figure 4A). The extension rates for the 211, 427, 836, and 1551 bp DNA molecules were pooled separately and fit to individual Gaussian distributions (Figure S4 of the Supporting Information). A length-dependent extension rate was observed (Figure 4C). The detailed parameters for assembly of Alba1 onto the dsDNA molecule are listed in Table 2.

**The Incoming-Strand TPM Experiment Was Used To Verify the Alba1-Mediated DNA Condensation Mechanism.** The crystal structure and NMR data have supported the existence of dimer–dimer contacts between two Alba nucleoprotein filaments, implying that dimer–dimer contacts play an important role in DNA condensation.<sup>10,12</sup> Recently, Laurens et al. found that there are different protein–protein interactions regulated by the Alba concentration and Alba variants.<sup>22</sup> It has been pointed out that Phe60 of Alba1 plays an important role in regulating the Alba1 dimer–Alba1 dimer interaction through either cooperative side-to-side binding along dsDNA molecules or interaction with dimers on an adjacent dsDNA molecule.<sup>22</sup> In this study, we used an incoming-strand TPM experiment to verify the existence of dimer–dimer contacts between two Alba1 nucleoprotein filaments at different Alba1 concentrations. A solution of incoming Alba1-coated 211 bp dsDNA molecules labeled with 200 nm polystyrene beads was loaded into a reaction chamber containing surface-immobilized Alba1-coated 211 bp dsDNA molecules. In this system, the appearance of tethered beads signaled the formation of dimer–dimer contacts between two Alba1 nucleoprotein filaments. According to Stokes–Einstein

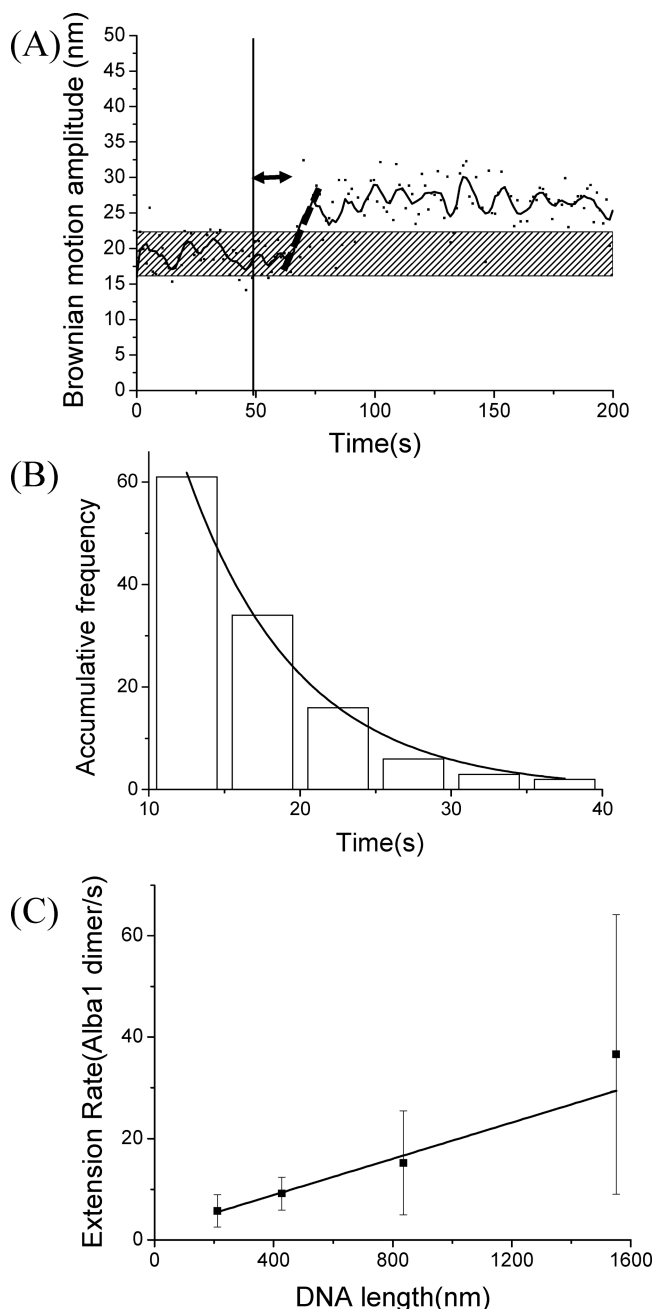


**Figure 4.** Kinetic analysis of the BM time trace. (A) BM time trace of a 211 bp DNA molecule in response to the addition of 1  $\mu\text{M}$  Alba1. The black lines indicate the addition of Alba1. The hatched bar indicates the average BM value of bare 211 bp DNA molecules. The double-headed line indicates the nucleation time, representing the DNA binding affinity of Alba1. The dashed line indicates continuous Alba1 nucleoprotein filament formation. (B) The distribution of the nucleation time, indicated by the double-headed line in panel A, was pooled to construct a histogram, and the rate constants were determined by fitting to a single-exponential decay algorithm ( $R^2 = 0.99$ ;  $T = 7.4 \pm 0.4$  s;  $N = 61$ ). (C) The extension rate vs the DNA length was fit to a straight line using the equation  $y = 0.025x$  ( $R^2 = 0.99$ ). The error bar represents the 68% CL.

equation, the diffusion coefficient of a polystyrene bead with a diameter of 220 nm is  $2.21 \mu\text{m}^2/\text{s}$  at  $22^\circ\text{C}$  and the time required for a 200 nm polystyrene bead to diffuse out of the focus plane is  $\sim 110$  ms.<sup>36</sup> Tethered molecules that persisted for over five frames were chosen for the lifetime analysis, which

**Table 2.** Detailed Kinetic Parameters for the Interaction between Alba1 and DNA Molecules

DNA substrate (bp)	nucleation rate (bp/s)	extension rate (no. of Alba1 dimers/s)	BM plateau value (nm)
211	$(6.4 \pm 0.3) \times 10^4$	$5.75 \pm 3.18$	$26.1 \pm 5.4$
427	not determined	$9.15 \pm 3.25$	$54.4 \pm 8.1$
836	not determined	$15.23 \pm 10.27$	$107.0 \pm 15.6$
1551	not determined	$36.64 \pm 27.59$	$180.4 \pm 24.5$

represents the stability of the interactions between these two nucleoprotein filaments.

A control experiment was performed using two bare dsDNA molecules in the absence of Alba1. Only very few tethering events were observed. The typical BM time trace persisted for  $< 2$  s, as shown in panel (i) of Figure S5 of the Supporting Information. The lifetime histogram of this control experiment was fit to a single-exponential decay, returning an average lifetime of  $2.0 \pm 0.1$  s [Figure 5, (i)], representing the

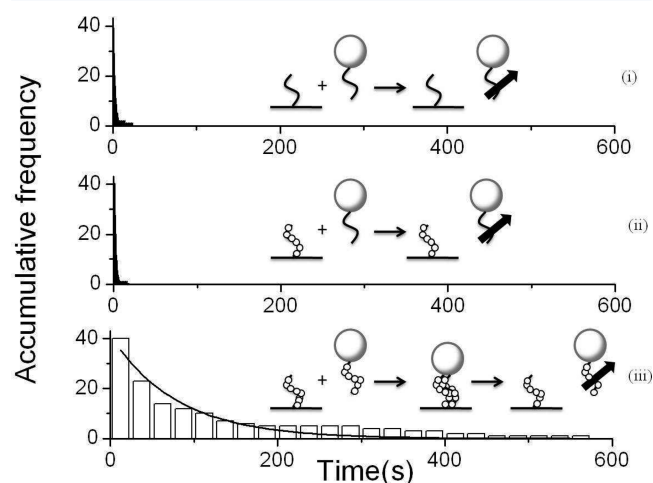


**Figure 5.** Incoming-strand experiment to verify the possible mechanism of Alba1-induced DNA condensation. (i) Lifetime histogram for tethers formed between bare 211 bp DNA molecules and surface-bound 211 bp DNA molecules in the absence of Alba1. The data were fit to a single-exponential curve, with a time constant of  $2.0 \pm 0.1$  s. (ii) Lifetime histogram of the tethers formed between bare 211 bp DNA molecules and surface-bound 211 bp DNA molecules preincubated with  $10 \mu\text{M}$  Alba1 for 30 min. The data were fit to a single-exponential curve, with a time constant of  $1.6 \pm 0.1$  s. (iii) Lifetime histogram of the tethers formed between Alba1-bound 211 bp DNA molecules and surface-bound 211 bp DNA molecules preincubated with  $10 \mu\text{M}$  Alba1 for 30 min. The data were fit to a single-exponential curve with a time constant of  $79.8 \pm 8.0$  s. The insets illustrate the reaction conditions for the three conditions described above. The white sphere represents the streptavidin-labeled 200 nm polystyrene bead. The white spots represent the Alba1 molecules. The black curve represents the DNA molecules. The arrowed black line indicates the dissociation of the nucleoprotein complex. The error bar expresses the 95% CL.

nonspecific interaction between streptavidin on the surface of a polystyrene bead and the glass surface, which confirms that there are no specific interactions between two bare dsDNA molecules in this system, as expected. Subsequently,  $10 \mu\text{M}$  Alba1 was loaded into a reaction chamber to incubate with immobilized 211 bp dsDNA molecules for 30 min, allowing for the formation of complete Alba1-bound nucleoprotein



filaments. Before the incoming bead-labeled 211 bp dsDNA molecules had been loaded in the absence of Alba1, 100  $\mu$ L of reaction buffer without Alba1 was used to wash all free Alba1 from the chamber. The appearance of tethered molecules was analyzed following the same criteria described above. A typical BM time trace and the corresponding lifetime histogram are shown in panel (ii) of Figure S5 of the Supporting Information and panel (ii) of Figure 5, respectively, with an average lifetime of  $1.6 \pm 0.1$  s. The short lifetime of this control experiment indicates that individual Alba1 nucleoprotein filaments cannot bind with another bare dsDNA molecule, suggesting that each Alba1 only has one dsDNA binding site. Finally, both incoming bead-labeled 211 bp dsDNA molecules and surface-bound 211 bp dsDNA molecules were preincubated with 10  $\mu$ M Alba1 separately for 30 min before the initiation of the incoming-strand TPM experiment. In this case, tethers appeared and persisted for  $>70$  s, with a typical BM time trace shown in panel (iii) of Figure S5 of the Supporting Information. An average lifetime of  $79.8 \pm 8.0$  s was observed in this experiment [Figure 5, (iii)], which suggests the existence of transient dimer–dimer contacts between two Alba1 nucleoprotein filaments at Alba1 concentrations above the  $K_d$ . The significant intersegment bridges have been reported at relatively low Alba1 concentrations (1–100 nM).<sup>22</sup> Therefore, the same experimental procedure was conducted at Alba1 concentrations below the  $K_d$  to investigate the existence of intersegment bridges. Both incoming bead-labeled 211 bp dsDNA molecules and surface-bound 211 bp dsDNA molecules were preincubated with 100 nM Alba1 separately for 30 min before the initiation of the incoming-strand TPM experiment. Different from the  $K_d$  Alba1 condition described above (10  $\mu$ M Alba1) under which transient tethers formed with an average lifetime of  $79.8 \pm 8.0$  s, the stable tethering that persisted even after extensive buffer wash was observed at Alba1 concentrations below the  $K_d$  (100 nM Alba1) [Figure S5 of the Supporting Information, (iv)]. This suggests the existence of stable dimer–dimer interactions, formed between short Alba1 nucleoprotein segments, at Alba1 concentrations below the  $K_d$ .

## DISCUSSION

We used single-molecule TPM and OT experiments to study the interaction between Alba1 and DNA molecules and the concentration-dependent Alba1 dimer–Alba1 dimer interaction. Using TPM experiments, an increase in the BM amplitude, representing the stiffness of dsDNA, was observed at Alba1 concentrations above the  $K_d$  (Figure 1). Although it has been shown that Alba1 nucleoprotein filaments can form a tangled, stem–loop structure at Alba1 concentrations below the  $K_d$ ,<sup>8,22</sup> this study found no detectable decrease in the BM amplitude at Alba1 concentrations of  $<100$  nM. This discrepancy could be explained by the fact that the DNA molecules used here are too short to form the stable stem–loop structure. For better spatial resolution, the DNA molecules used in the TPM experiment were smaller than 500 bp.<sup>37</sup> Although Alba1–Alba1 interactions have been observed between these short Alba1 nucleoprotein segments, the steric hindrance of tethered beads and the rigidity of DNA molecules could potentially destabilize the loop formation.<sup>38</sup> Once the concentration of Alba1 was greater than 1  $\mu$ M, an apparent increase in the BM amplitude was observed, and the change in the BM amplitude approached constant BM plateau values of  $25.7 \pm 5.6$  and  $26.1 \pm 5.4$  nm for Alba1 nucleoprotein filaments at 1 and 10  $\mu$ M, respectively. The similarity of these average

BM plateau values suggests that there is no intermediate BM plateau value for Alba1 nucleoprotein filaments. This finding supports the hypothesis that the Alba1 assembly process is continuous and highly cooperative at Alba1 concentrations above the  $K_d$  (Figure S1 of the Supporting Information).

It has been reported that there is only small change in the persistence length of Alba1 nucleoprotein filaments at Alba1 concentrations below the  $K_d$  in which the contour length of the filament remains the same.<sup>22</sup> The BM amplitude change in the TPM setup results from two factors: a change in the contour length and a change in the persistence length. Our OT study confirmed that the persistence length of Alba1 nucleoprotein filaments increases but that the contour length remains the same under our experimental condition. Because there are only small changes in the persistence length at Alba1 concentrations below the  $K_d$ , it is possible that we did not see the BM change because of the resolution limits of the TPM setup. It has been reported that stable interactions occur between small Alba1-bound segments at Alba1 concentrations below the  $K_d$ .<sup>22</sup> In the incoming-strand TPM experiments, stable tethering was observed at 100 nM Alba1, and most tethers ( $>85\%$ ) persisted even after buffer wash, indicating that most DNA molecules contained only small Alba1-bound segments. This phenomenon is in accordance with our observation from the TPM experiment of no detectable change in the BM amplitude of the DNA molecules incubated with 100 nM Alba1. It is likely that at low concentrations (100 nM), Alba1 does bind to DNA but forms only small Alba1–DNA segments that cannot be detected by our TPM system.

The detailed kinetic analysis of the BM time trace provided two parameters, the nucleation time and extension rate, which reflect the DNA binding affinity of Alba1 and the polymerization capability of Alba1, respectively. The nucleation time will become shorter as the number of possible nucleation sites increases. In our current setup, a mixing time of 5 s limited our time resolution. Therefore, any nucleation process faster than 5 s was unable to be defined accurately. On the basis of a simple bimolecular collision model, the nucleation time distribution can be fit to a single-exponential decay model with a pseudo-first-order rate constant of  $(1.3 \pm 0.0_6) \times 10^{-1} \text{ s}^{-1}$  and a normalized association rate constant of  $(6.4 \pm 0.3) \times 10^{-4} \text{ bp}^{-1} \text{ s}^{-1}$ . Using the normalized association rate constant obtained here, detectable nucleation events are limited to DNA molecules of fewer than 313 bp. This is consistent with our results, which showed that nucleation events are detectable only with 211 bp DNA in our current system.

For the DNA molecule, the continuous increase in the BM amplitude in response to the addition of Alba1 was fit with a straight line, and the slope represented the extension rate, reflecting the polymerization ability of Alba1. Recently, isothermal titration calorimetry, 4',6-diamidino-2-phenylindole (DAPI) dye displacement, and gel electrophoresis studies have suggested a binding stoichiometry of approximately 6 bp of DNA per Alba1 dimer.<sup>7</sup> If the plateau in the BM time trace represents the fully assembled Alba1 nucleoprotein filament, the extension rate can be represented as an Alba1 dimer assembly rate of  $5.7 \pm 0.5$  Alba1 dimers/s for 211 bp DNA molecules at a concentration of 1  $\mu$ M. The normalized extension rate obtained from the slope is  $(2.5 \pm 0.0_1) \times 10^{-2}$  Alba1 dimers  $\text{bp}^{-1} \text{ s}^{-1}$  (Figure 4C). Interestingly, a length-dependent extension rate was observed (Figure 4C). One possible mechanism for explaining the length-dependent extension rate is that the number of nucleation sites increases

as the length of the dsDNA increases, whereas the polymerization rate remains constant. This finding is consistent with our nucleation time analysis results, in which the nucleation was faster when the DNA molecule became longer. Even though the poor resolution of our TPM system is expected to return with a lower binding constant, the determined binding constant indeed places a lower limit, offering important kinetic parameters for Alba1–DNA interaction. The Lys16 residue of Alba1 is important in DNA binding, and the Phe60 residue of Alba1 plays an important role in the protein–protein interaction.<sup>22</sup> In addition, histone acetyltransferases (HATs) and other DNA-binding proteins, such as Sso10b2 and Sac7d in archaea, are known to regulate the DNA binding affinity of Alba1. The TPM experiment developed here can be used to study how the change in these residues or the presence of other DNA-binding proteins could affect either the DNA affinity or polymerization of Alba1 in the future.

In previous studies, formation of the stem–loop structure was observed at Alba1 concentrations below the  $K_d$ .<sup>9</sup> This structure has been suggested to be composed of two Alba1 nucleoprotein filaments based on EM analysis.<sup>8</sup> A growing body of evidence supports the assumption that dimer–dimer contacts include the hydrophobic interactions within conserved  $\alpha 1$  helices and the two well-known hydrogen bonding interactions.<sup>10,12,22</sup> In this study, the incoming-strand TPM experiments offer direct evidence that there are stable dimer–dimer contacts between two Alba1 nucleoprotein filaments and that this interaction pulls the two dsDNA molecules together at Alba1 concentrations below the  $K_d$ , consistent with previous observations.<sup>22</sup> Because no stable tethers were observed in the control experiment performed between an Alba1 nucleoprotein filament and a bare dsDNA molecule, Alba1 likely possesses only one DNA-binding site, and this binding site is different from the contact points between Alba1 nucleoprotein filaments. The presence of transient dimer–dimer contacts at Alba1 concentrations above the  $K_d$  was also observed, but the interaction was weaker and relatively short-lived, with an average lifetime of approximately  $79.8 \pm 8.0$  s. The phenomenon has not been observed using an optical unzipping experiment. The inconsistency could be that only the stable interaction is detected in the optical unzipping system. Therefore, no interaction at Alba1 concentrations above the  $K_d$  was reported by Laurens et al.<sup>22</sup> However, not only the stable interaction but also the transient interactions can be observed in the incoming-strand TPM experiment. Moreover, the average stability of transient interactions can be determined in the incoming-strand TPM experiments, highlighting its ability to study the weak and transient interactions.

Combining previous studies and the results observed here, we depict one possible model for the interaction between Alba1 and dsDNA molecules in Figure S6 of the Supporting Information.<sup>8,9,22</sup> At Alba1 concentrations below the  $K_d$ , a partial shortening of the DNA length can be observed, which has been pointed out in the previous studies.<sup>9,22</sup> The stable dimer–dimer contacts between two distant regions covered by Alba1 can play a role in stabilizing formation of the stem–loop structure within the same DNA. As the concentration of Alba1 is increased, the Alba1 filaments will become elongated, eventually covering the whole dsDNA, and switch to the weaker dimer–dimer contacts, verified in the incoming-strand TPM experiment. This occurs via addition of Alba1 to the original nucleation sites rather than by random binding at the other sites along the dsDNA. The increased persistence length

will stiffen the DNA molecule and break any stem–loop conformation. Therefore, the increased rigidity of the Alba1 nucleoprotein filament at Alba1 concentrations above the  $K_d$  results in no significant DNA compaction. Previous studies have shown that a smaller DNA-binding protein, Sac7d, is able to bind to the DNA minor groove and causes a kink on the DNA strand of approximately  $60^\circ$ . A significant DNA condensation of a Sac7d nucleoprotein filament was observed with this mechanism.<sup>8,39</sup> Alba1, one of the most abundant DNA-binding proteins in *S. acidocaldarius*, has long been implicated as a possible architectural DNA-binding protein. It is possible that Alba1-mediated DNA compaction mechanisms may involve interactions with other DNA-binding proteins, such as Sso10b2, Sac7d, and histone acetyltransferases (HATs), to achieve architectural regulation of DNA. Thus, these proteins together may play a variety of different roles in assisting archaeal DNA packaging. Further studies of the interaction of Alba1 and DNA molecules in the presence of other DNA-binding proteins are likely to contribute to our understanding of chromatin organization in archaea.

## CONCLUSIONS

A fast Alba1 nucleation rate on dsDNA molecules of approximately  $(6.4 \pm 0.3) \times 10^{-4} \text{ bp}^{-1} \text{ s}^{-1}$  is consistent with a high DNA affinity. Moreover, the Alba1 concentration-independent BM plateau value upon addition of Alba1 confirms the highly cooperative nature of the Alba1–DNA interaction, with an extension rate of  $(2.5 \pm 0.01) \times 10^{-2} \text{ Alba1 dimers bp}^{-1} \text{ s}^{-1}$ . The OT results confirmed that a 5-fold increase in the persistence length of the Alba1 nucleoprotein filament is the major cause for the increase in the BM amplitude of DNA molecule in response to the Alba1, while the contour length remained unchanged at Alba1 concentrations above the  $K_d$ . Furthermore, the presence of significant dimer–dimer contacts between two Alba1 nucleoprotein filaments is regulated by the concentration of Alba1, as shown in the incoming-strand TPM experiments. The single-molecule experiments presented here are powerful tools for investigating the properties and functions of Alba1. Future experiments to study Alba variants, other small DNA-binding proteins, and HATs will help unveil the mechanisms involved in chromatin organization and gene regulation in archaea.

## ASSOCIATED CONTENT

### Supporting Information

Supplementary Figures S1–S6. This material is available free of charge via the Internet at <http://pubs.acs.org>.

## AUTHOR INFORMATION

### Corresponding Author

\*E-mail: [hffan2@ym.edu.tw](mailto:hffan2@ym.edu.tw). Telephone: 886-2-28267941. Fax: 886-2-28234898.

### Funding

This work was supported by the National Science Council of Taiwan (101-2113-M-010-005-MY2) and National Yang Ming University, which provided support to H.-F.F. H.-W.L. was supported by the National Science Council of Taiwan (100-2113-M-002-009-MY2) and the National Taiwan University. C.-H.H. has received grants (ERP-101R8600 and NTU-ICRP-102R7560-5) from the Excellent Research Projects of National Taiwan University.



# Notes

The authors declare no competing financial interest.

# REFERENCES

- (1) Luger, K., Mader, A. W., Richmond, R. K., Sargent, D. F., and Richmond, T. J. (1997) Crystal structure of the nucleosome core particle at 2.8 Å resolution. *Nature* 389, 251–260.
- (2) Sandman, K., Pereira, S. L., and Reeve, J. N. (1998) Diversity of prokaryotic chromosomal proteins and the origin of the nucleosome. *Cell. Mol. Life Sci.* 54, 1350–1364.
- (3) Sandman, K., Soares, D., and Reeve, J. N. (2001) Molecular components of the archaeal nucleosome. *Biochimie* 83, 277–281.
- (4) Xue, H., Guo, R., Wen, Y., Liu, D., and Huang, L. (2000) An abundant DNA binding protein from the hyperthermophilic archaeon *Sulfolobus shibatae* affects DNA supercoiling in a temperature-dependent fashion. *J. Bacteriol.* 182, 3929–3933.
- (5) Forterre, P., Confalonieri, F., and Knapp, S. (1999) Identification of the gene encoding archeal-specific DNA-binding proteins of the Sac10b family. *Mol. Microbiol.* 32, 669–670.
- (6) Bell, S. D., Botting, C. H., Wardleworth, B. N., Jackson, S. P., and White, M. F. (2002) The interaction of Alba, a conserved archaeal chromatin protein, with Sir2 and its regulation by acetylation. *Science* 296, 148–151.
- (7) Wardleworth, B. N., Russell, R. J., Bell, S. D., Taylor, G. L., and White, M. F. (2002) Structure of Alba: An archaeal chromatin protein modulated by acetylation. *EMBO J.* 21, 4654–4662.
- (8) Lurz, R., Grote, M., Dijk, J., Reinhardt, R., and Dobrinski, B. (1986) Electron microscopic study of DNA complexes with proteins from the Archaeobacterium *Sulfolobus acidocaldarius*. *EMBO J.* 5, 3715–3721.
- (9) Jelinska, C., Conroy, M. J., Craven, C. J., Hounslow, A. M., Bullough, P. A., Waltho, J. P., Taylor, G. L., and White, M. F. (2005) Obligate heterodimerization of the archaeal Alba2 protein with Alba1 provides a mechanism for control of DNA packaging. *Structure* 13, 963–971.
- (10) Tanaka, T., Padavattan, S., and Kumarevel, T. (2012) Crystal structure of archaeal chromatin protein Alba2-double-stranded DNA complex from *Aeropyrum pernix* K1. *J. Biol. Chem.* 287, 10394–10402.
- (11) Crnigoj, M., Podlesek, Z., Zorko, M., Jerala, R., Anderluh, G., and Ulrikh, N. P. (2013) Interactions of archaeal chromatin proteins Alba1 and Alba2 with nucleic acids. *PLoS One* 8, e58237.
- (12) Jelinska, C., Petrovic-Stojanovska, B., Ingledew, W. J., and White, M. F. (2010) Dimer-dimer stacking interactions are important for nucleic acid binding by the archaeal chromatin protein Alba. *Biochem. J.* 427, 49–55.
- (13) Sandman, K., and Reeve, J. N. (2005) Archaeal chromatin proteins: Different structures but common function? *Curr. Opin. Microbiol.* 8, 656–661.
- (14) Dohoney, K. M., and Gelles, J. (2001) chi-Sequence recognition and DNA translocation by single RecBCD helicase/nuclease molecules. *Nature* 409, 370–374.
- (15) Hua, W., Chung, J., and Gelles, J. (2002) Distinguishing inchworm and hand-over-hand processive kinesin movement by neck rotation measurements. *Science* 295, 844–848.
- (16) Perkins, T. T., Li, H.-W., Dalal, R. V., Gelles, J., and Block, S. M. (2004) Forward and Reverse Motion of Single RecBCD Molecules on DNA. *Biophys. J.* 86, 1640–1648.
- (17) Svoboda, K., Schmidt, C. F., Schnapp, B. J., and Block, S. M. (1993) Direct observation of kinesin stepping by optical trapping interferometry. *Nature* 365, 721–727.
- (18) Yasuda, R., Noji, H., Kinosita, K., and Yoshida, M. (1998) F-1-ATPase is a highly efficient molecular motor that rotates with discrete 120° steps. *Cell* 93, 1117–1124.
- (19) Strick, T. R., Croquette, V., and Bensimon, D. (2000) Single-molecule analysis of DNA uncoiling by a type II topoisomerase. *Nature* 404, 901–904.
- (20) Tanaka, H., Homma, K., Iwane, A. H., Katayama, E., Ikebe, R., Saito, J., Yanagida, T., and Ikebe, M. (2002) The motor domain determines the large step of myosin-V. *Nature* 415, 192–195.
- (21) Dumont, S., Cheng, W., Serebrov, V., Beran, R. K., Tinoco, I., Pyle, A. M., and Bustamante, C. (2006) RNA translocation and unwinding mechanism of HCVNS3 helicase and its coordination by ATP. *Nature* 439, 105–108.
- (22) Laurens, N., Driessen, R. P., Heller, I., Vorselen, D., Noom, M. C., Hol, F. J., White, M. F., Dame, R. T., and Wuite, G. J. (2012) Alba shapes the archaeal genome using a delicate balance of bridging and stiffening the DNA. *Nat. Commun.* 3, 1328.
- (23) Fan, H. F., and Li, H. W. (2009) Studying RecBCD helicase translocation along Chi-DNA using tethered particle motion with a stretching force. *Biophys. J.* 96, 1875–1883.
- (24) Fan, H. F., Cox, M. M., and Li, H. W. (2011) Developing single-molecule TPM experiments for direct observation of successful RecA-mediated strand exchange reaction. *PLoS One* 6, e21359.
- (25) Hsu, H. F., Ngo, K. V., Chitteni-Pattu, S., Cox, M. M., and Li, H. W. (2011) Investigating *Deinococcus radiodurans* RecA protein filament formation on double-stranded DNA by a real-time single-molecule approach. *Biochemistry* 50, 8270–8280.
- (26) Zhao, H., Li, M., Wang, L., Su, Y., Fang, H., Lin, J., Mohabeer, N., and Li, D. (2012) Angiotensin II Induces TSLP via an AT1 Receptor/NF-κB Pathway, Promoting Th17 Differentiation. *Cell. Physiol. Biochem.* 30, 1383–1397.
- (27) Fan, H. F., Ma, C. H., and Jayaram, M. (2013) Real-time single-molecule tethered particle motion analysis reveals mechanistic similarities and contrasts of F1p site-specific recombinase with Cre and lambda Int. *Nucleic Acids Res.* 41, 7031–7047.
- (28) Hsu, C. H., and Wang, A. H. (2011) The DNA-recognition fold of Sso7c4 suggests a new member of SpoVT-AbrB superfamily from archaea. *Nucleic Acids Res.* 39, 6764–6774.
- (29) Mackay, D. T., Botting, C. H., Taylor, G. L., and White, M. F. (2007) An acetylase with relaxed specificity catalyses protein N-terminal acetylation in *Sulfolobus solfataricus*. *Mol. Microbiol.* 64, 1540–1548.
- (30) Neuman, K. C., and Block, S. M. (2004) Optical trapping. *Rev. Sci. Instrum.* 75, 2787–2809.
- (31) Marko, J. F., and Siggia, E. D. (1995) Stretching DNA. *Macromolecules* 28, 8759–8770.
- (32) Seol, Y., Li, J., Nelson, P. C., Perkins, T. T., and Betterton, M. D. (2007) Elasticity of short DNA molecules: Theory and experiment for contour lengths of 0.6–7 microm. *Biophys. J.* 93, 4360–4373.
- (33) Manghi, M., Tardin, C., Baglio, J., Rousseau, P., Salome, L., and Destainville, N. (2010) Probing DNA conformational changes with high temporal resolution by tethered particle motion. *Phys. Biol.* 7, 046003.
- (34) Han, L., Lui, B., Blumberg, S., Beausang, J., Nelson, P., and Phillips, R. (2009) Calibration of Tethered Particle Motion Experiments. In *Mathematics of DNA Structure, Function and Interactions*, Vol. 150, Springer, New York.
- (35) Sun, B., Johnson, D. S., Patel, G., Smith, B. Y., Pandey, M., Patel, S. S., and Wang, M. D. (2011) ATP-induced helicase slippage reveals highly coordinated subunits. *Nature* 478, 132–135.
- (36) Einstein, A. (1956) *Investigations on the Theory of the Brownian Movement*, Dover Publications, Mineola, NY.
- (37) Fan, H. F. (2012) Real-time single-molecule tethered particle motion experiments reveal the kinetics and mechanisms of Cre-mediated site-specific recombination. *Nucleic Acids Res.* 40, 6208–6222.
- (38) Pinkney, J. N., Zawadzki, P., Mazuryk, J., Arciszewska, L. K., Sherratt, D. J., and Kapanidis, A. N. (2012) Capturing reaction paths and intermediates in Cre-loxP recombination using single-molecule fluorescence. *Proc. Natl. Acad. Sci. U.S.A.* 109, 20871–20876.
- (39) Robinson, H., Gao, Y. G., McCrary, B. S., Edmondson, S. P., Shriver, J. W., and Wang, A. H. (1998) The hyperthermophile chromosomal protein Sac7d sharply kinks DNA. *Nature* 392, 202–205.